Supplement of Eur. J. Mineral., 38, 179–195, 2026
https://doi.org/10.5194/ejm-38-179-2026-supplement

European Journal of Mineralogy
Open Access

Supplement of

Hydrous partial melting in gabbros drilled at the Southwest Indian Ridge (ODP Hole 735B): evidence from microstructures at grain boundaries

Jürgen Koepke

Correspondence to: Jürgen Koepke (koepke@mineralogie.uni-hannover.de)

BSE images and EPMA profiles from samples showing microstructures indicative for hydrous partial melting

This study examined 29 gabbro samples taken from ODP core 735B, which was drilled into the Atlantis Bank at SWIR. The following BSE images and EPMA profiles demonstrate microstructures at grain boundaries and the typical plagioclase compositions indicative of hydrous partial melting that were identified in 14 of the samples examined. The mineral data of these samples, acquired using EPMA, are listed in Table 1. In all BSE images, the An-enriched plagioclase at grain boundaries can be identified by its lighter grey levels, in contrast to the darker primary plagioclase grains.

As microstructures indicating hydrous partial melting are difficult to find, this appendix provides a catalogue of 14 examples of how to identify these microstructures using BSE imaging alongside microanalytical tools. Therefore, the paper includes a 15-page appendix displaying a variety of typical microstructures in different forms and textures. It should be noted that some thin sections contain very few (<5) observed microstructures, whereas others contain dozens.

Abbreviations used: ol - olivine; cpx - clinopyroxene; opx - orthopyroxene; $plag_{pri}$ – primary plagioclase; $plag_{HPM}$ – plagioclase enriched in An content formed by hydrous partial melting reactions; am – amphibole; ox – FeTi oxide. Primary phases are labelled in black and white, while the phases produced by hydrous partial melting are labelled in yellow. See the captions for the individual figures for details.

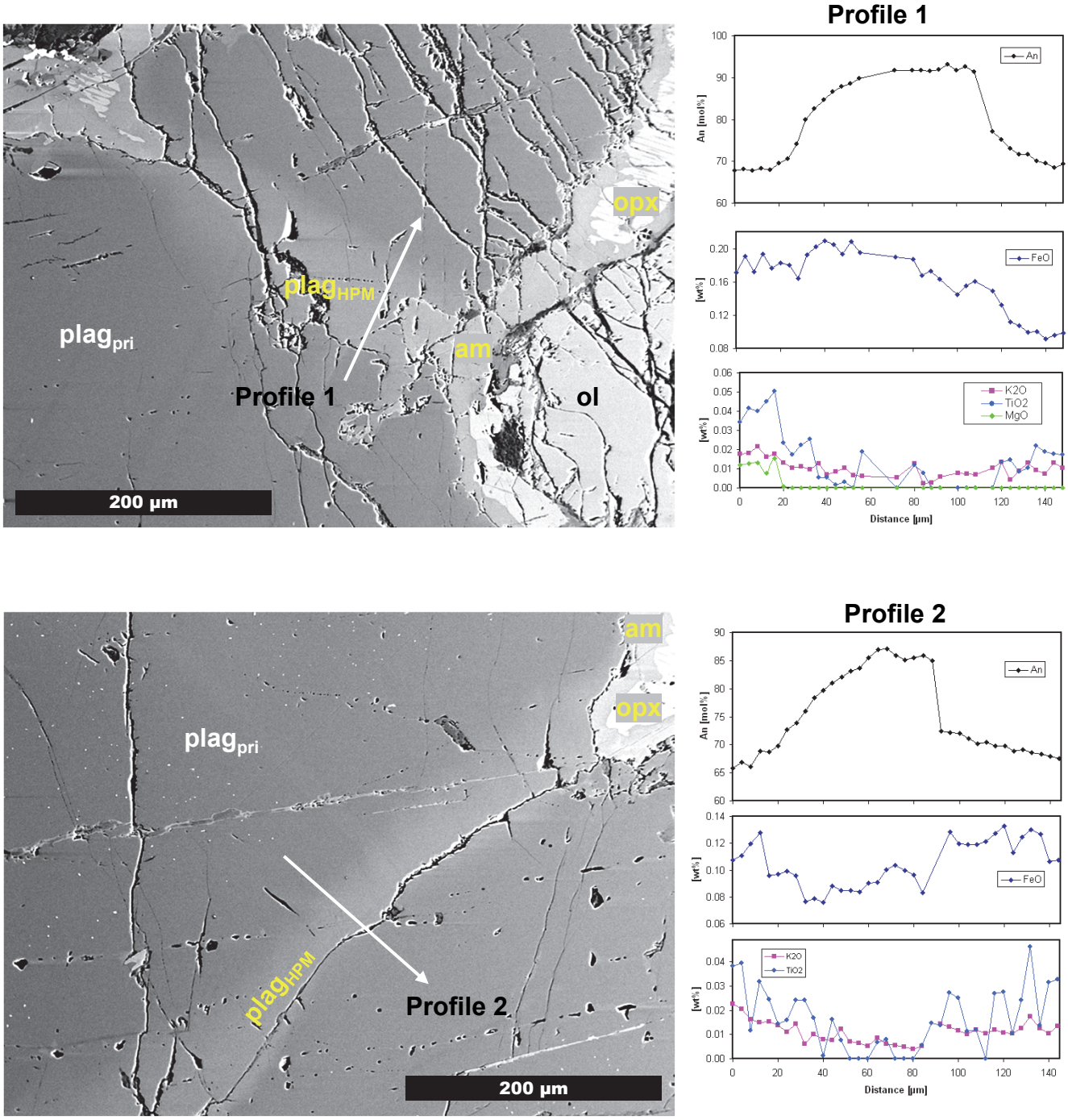

Figure S1. BSE images of zones of newly formed An-enriched plagioclase from gabbro 90-01-61-67, alongside related EPMA profiles. The coexisting mafic phases are pargasite and/or orthopyroxene. The An-rich zones are located directly at the grain boundary between primary plagioclase grains. Where the An-rich zones touch the mafic phases, orthopyroxene and amphibole corona textures develop. Note that the upper image shows that these zones are also locations of enhanced low-temperature hydrothermal alteration.

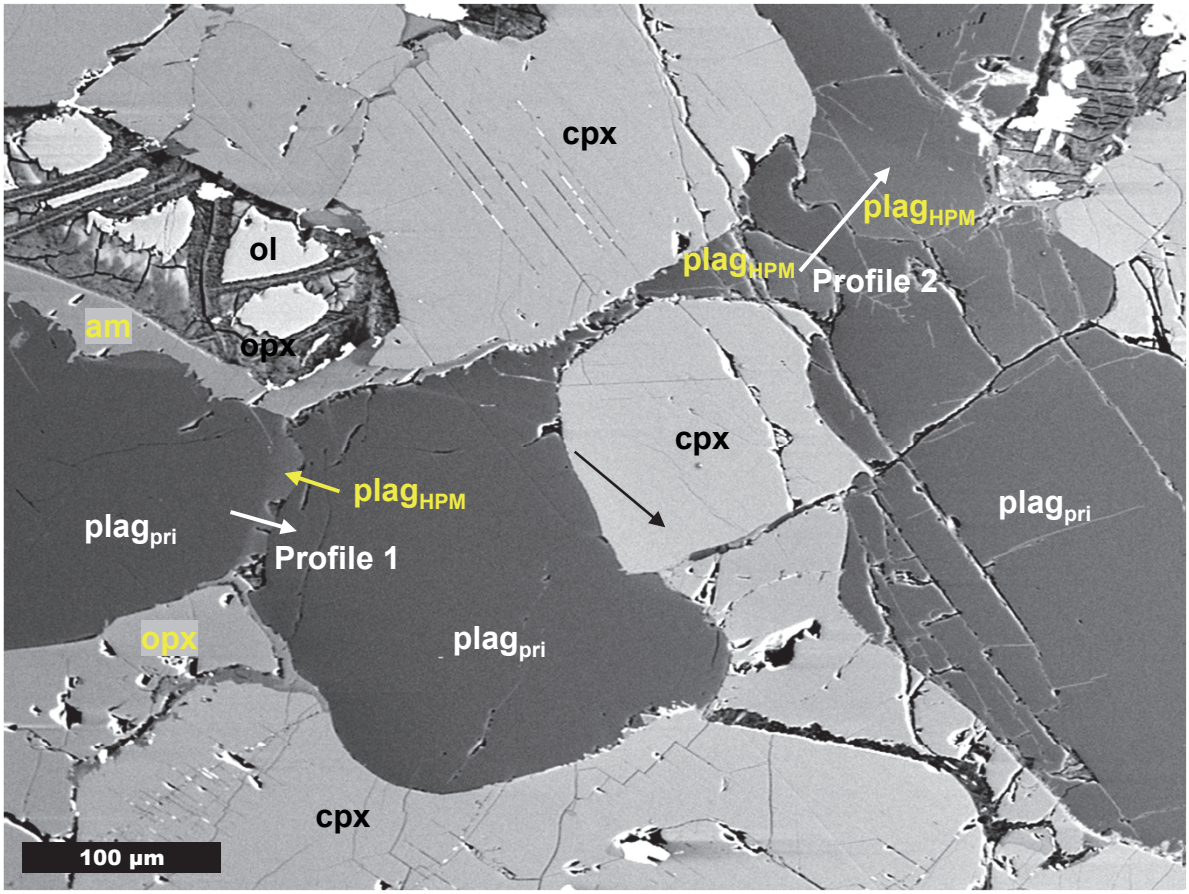

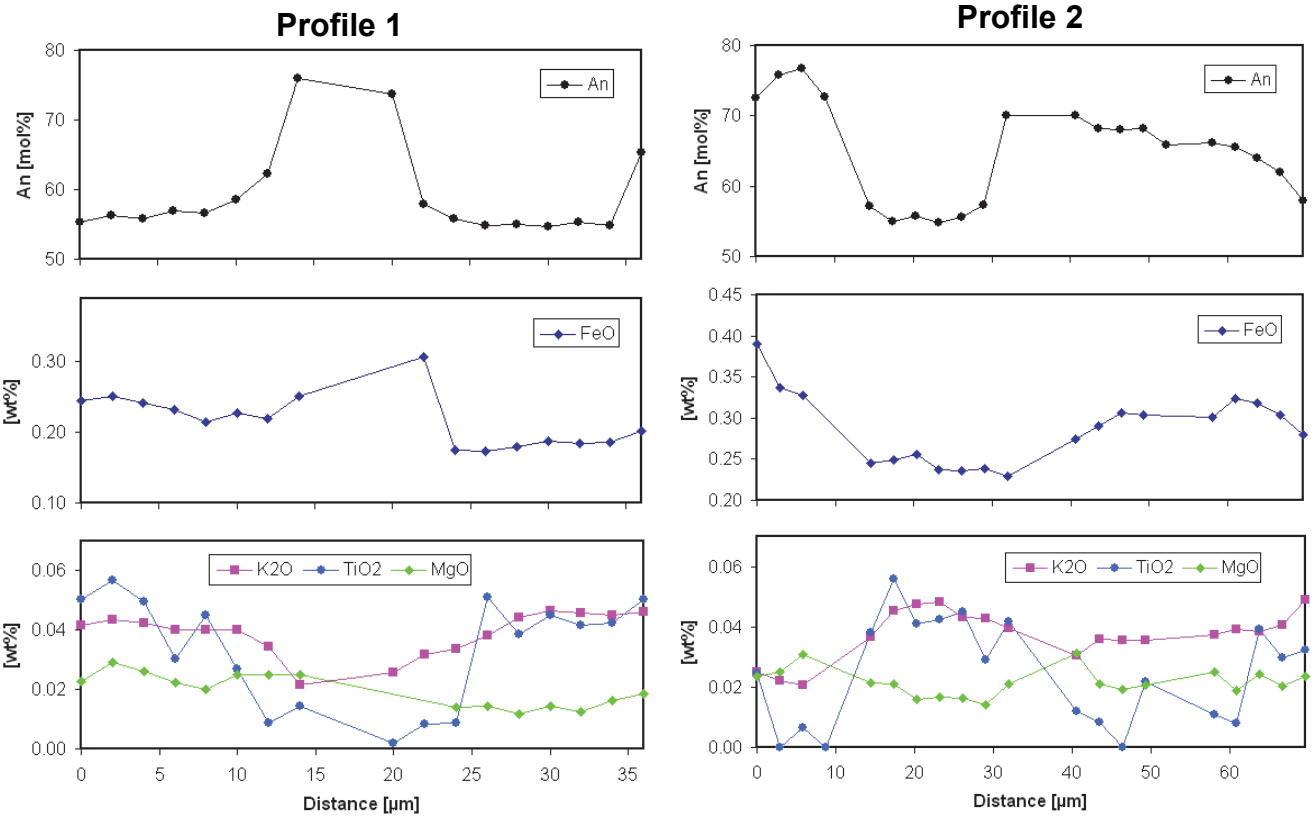

Figure S2. BSE image of zones of An-enriched plagioclase at grain boundaries between primary plagioclase and two related EPMA profiles in olivine gabbro 121-1-14-19. Since the An-rich zone of profile 1 is discontinuous, some unreliable analyses were obtained, resulting in few reliable data points. In the An-rich zones of both profiles, FeO is enriched while K_2O and TiO_2 are impoverished, in line with the general trend observed in other samples from SWIR. No characteristic trend is observed for MgO here.

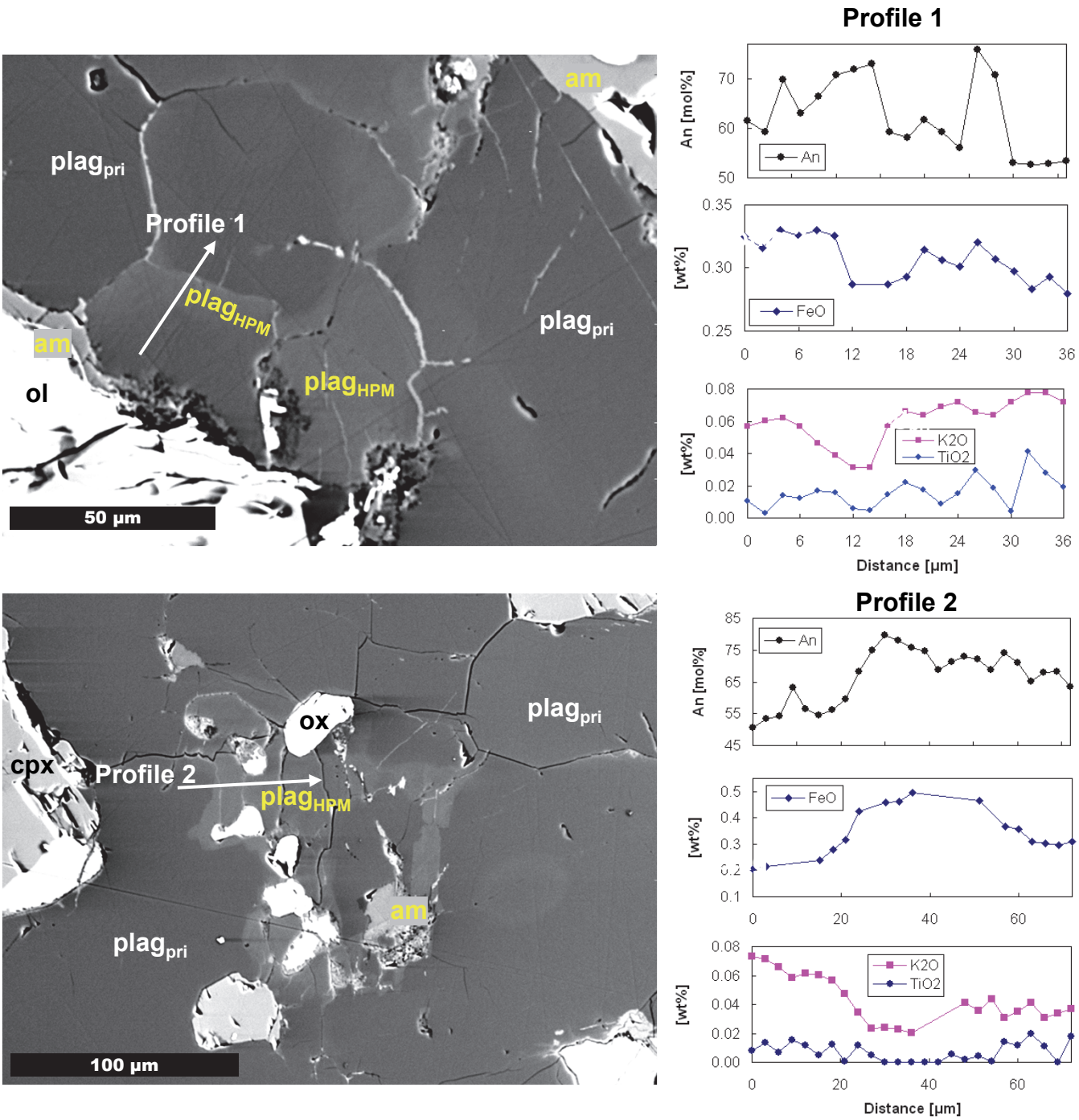

Figure S3. Two BSE images of zones of An-enriched plagioclase in olivine gabbro 137-6-112-119 and related EPMA profiles. The MgO content of most analyses is below the detection limit and is therefore not included in the trace element profiles. While the An-rich zone in the upper image developed from the boundaries between plagioclase grains, the zones in the lower image form neoblastic, patchy domains. The mafic phases that coexist with the An-enriched plagioclase are mainly pargasite and oxide.

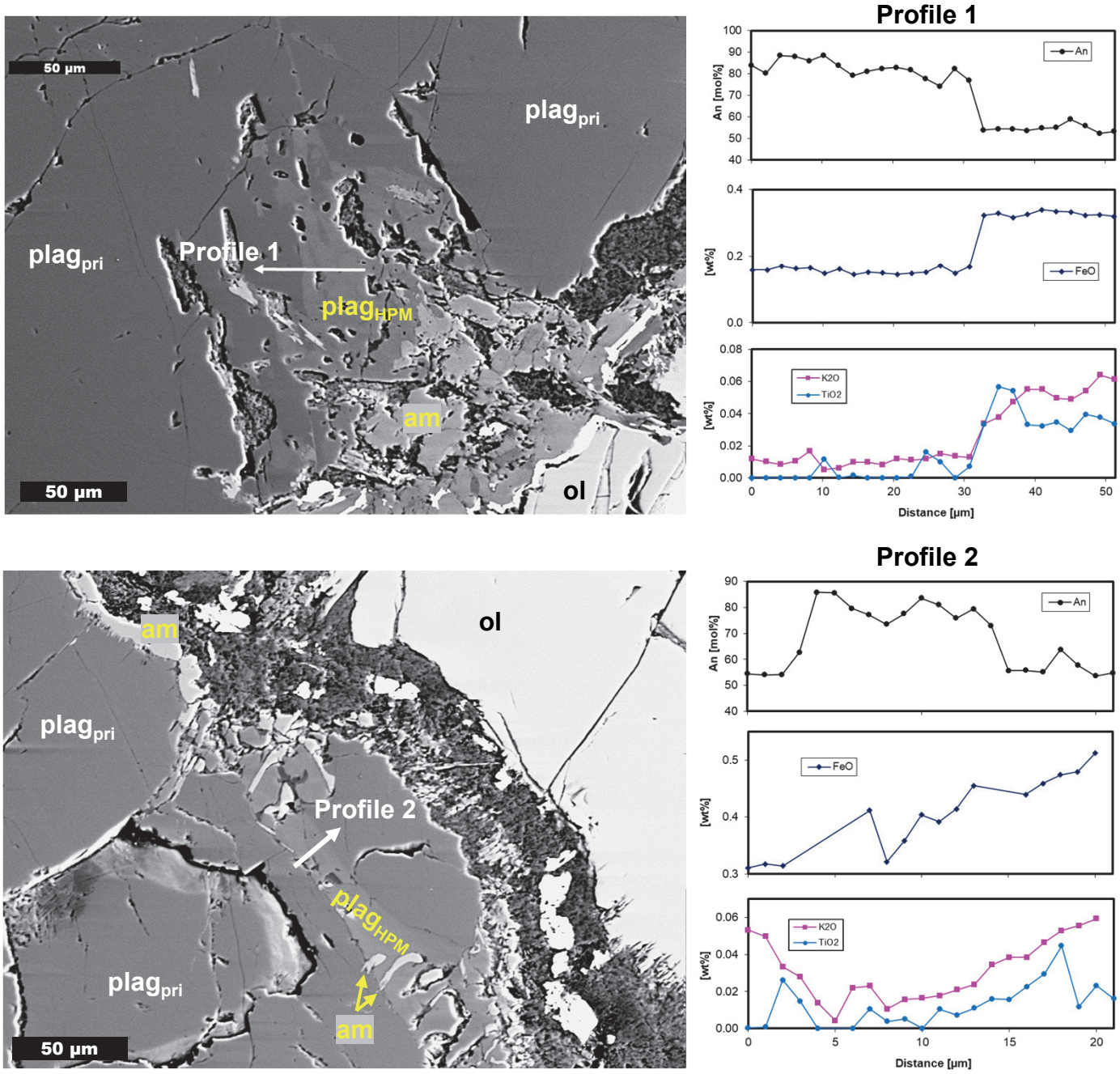

Figure S4. BSE images of zones of patchy An-enriched plagioclase domains within primary plagioclase, alongside two related EPMA profiles in olivine gabbro 142-1-114-120. Values of MgO are below the detection limit and therefore excluded from the profiles. Note the strong influence of secondary, low-temperature alteration. The formation temperature of an average pargasite within this sample was estimated to be 1017°C using the Ti-in-amphibole geothermometer of Ernst and Liu (1998), clearly indicating a formation in the magmatic stage.

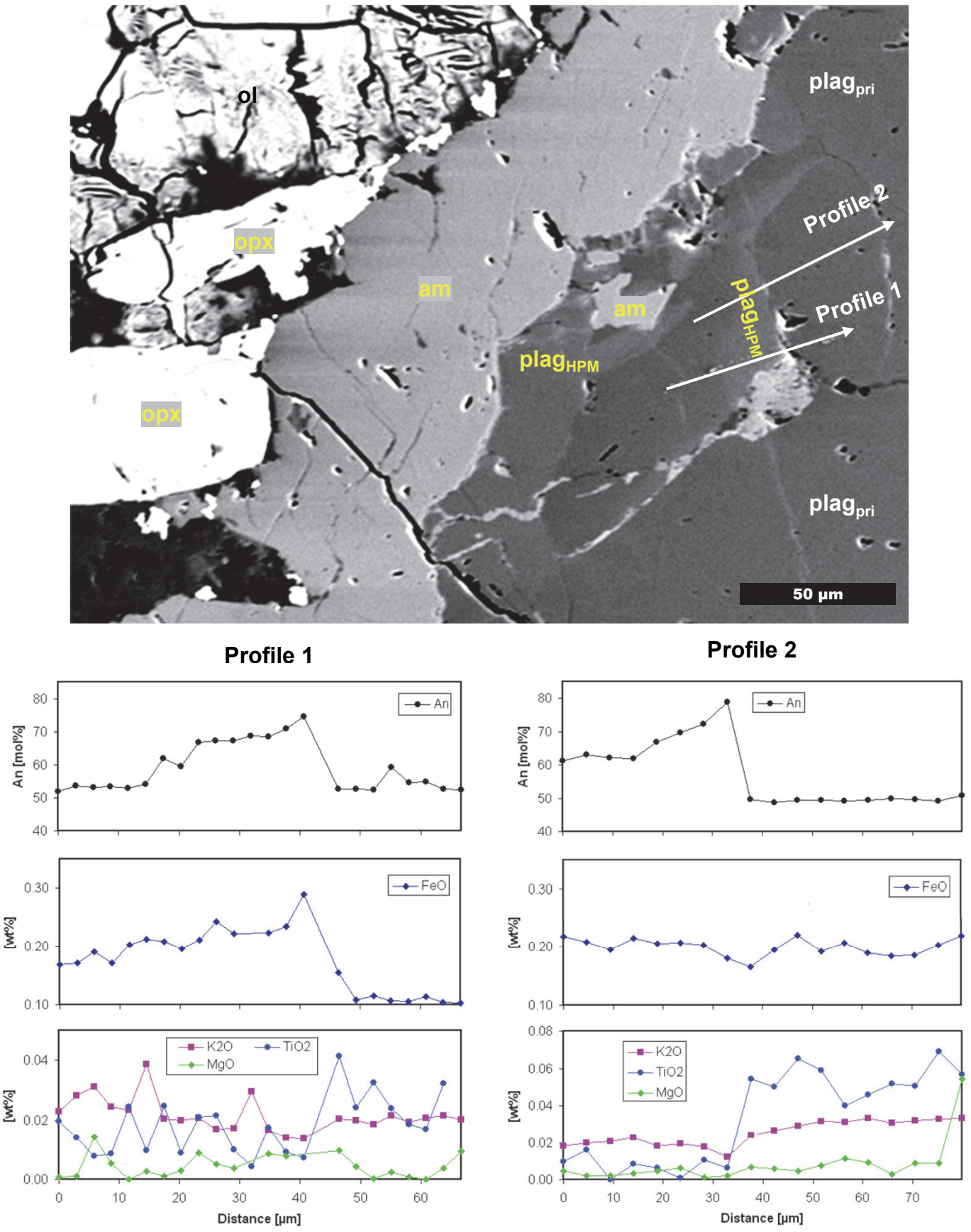

Figure S5. This BSE image shows zones of An-enriched plagioclase within primary plagioclase, together with two EPMA profiles across these zones. The newly formed plagioclase is in direct contact with magnesio-hastingsite, suggesting that these minerals grew together. Orthopyroxene is also part of this paragenesis and has formed interstitially between amphibole and strongly serpentinized primary olivine. The new An-rich plagioclases propagated from grain boundaries into the matrix plagioclase. The grain boundaries are also affected by secondary, low-temperature alteration. Sample: olivine gabbro 144-5-108-113.

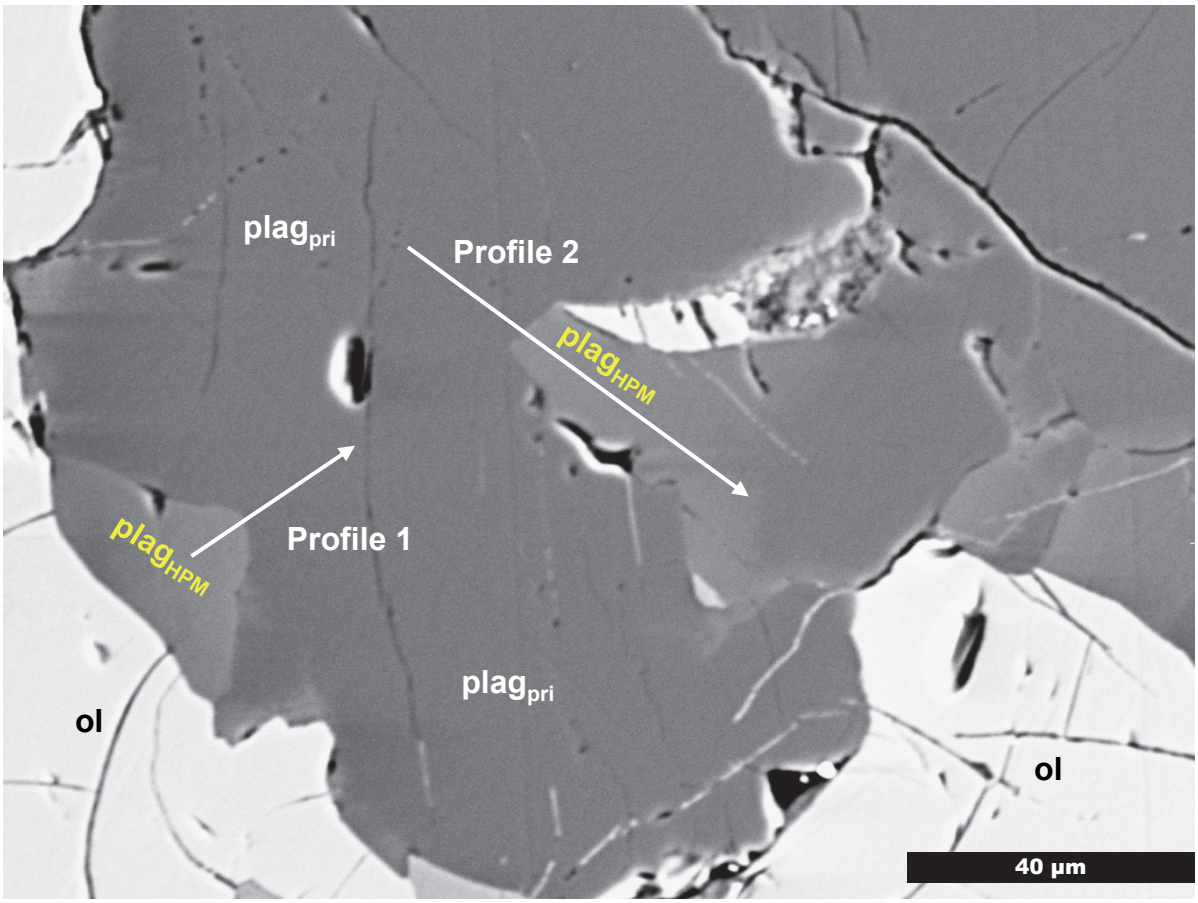

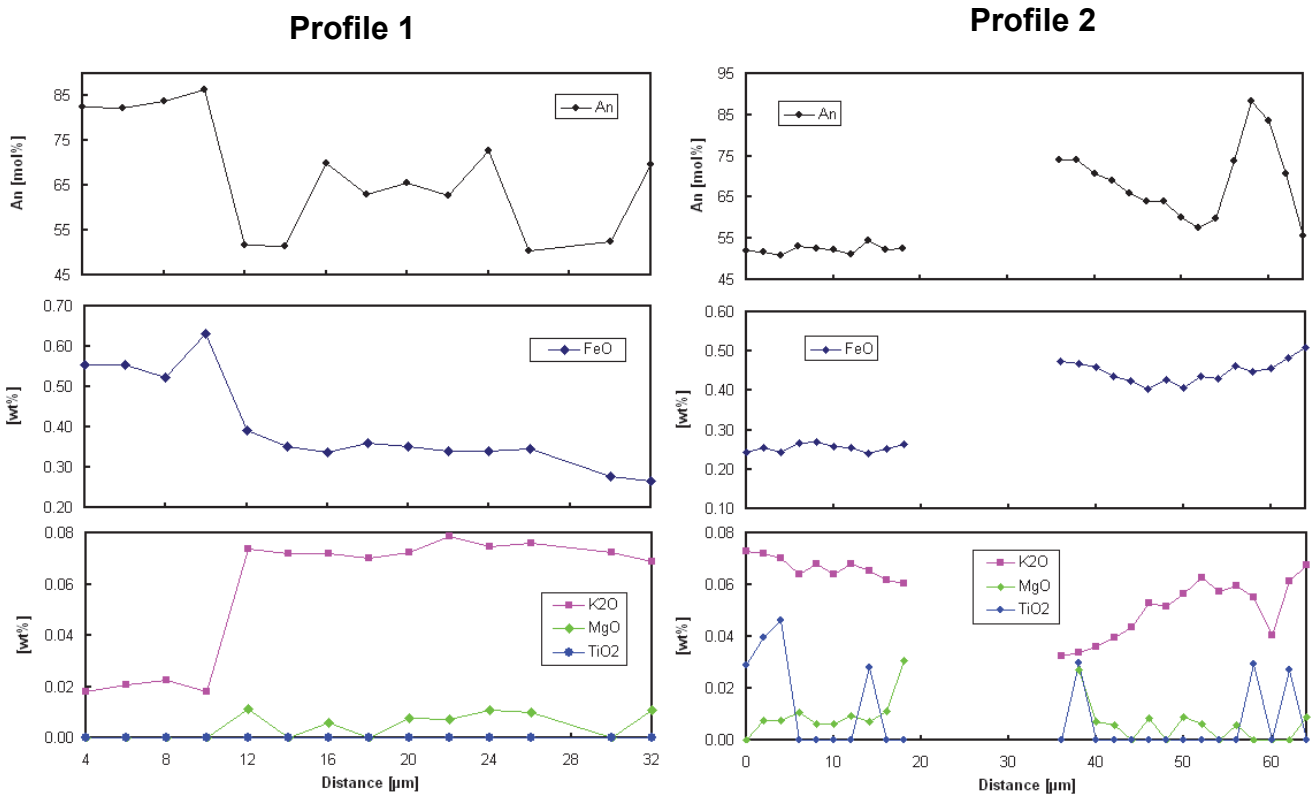

Figure S6. BSE image of zones of neoblastic An-enriched plagioclase developed at grain boundaries in primary plagioclase in olivine gabbro 149-2-61-65, alongside two EPMA profiles across these zones. The gap in profile 2's data set is due to unacceptable analyses.

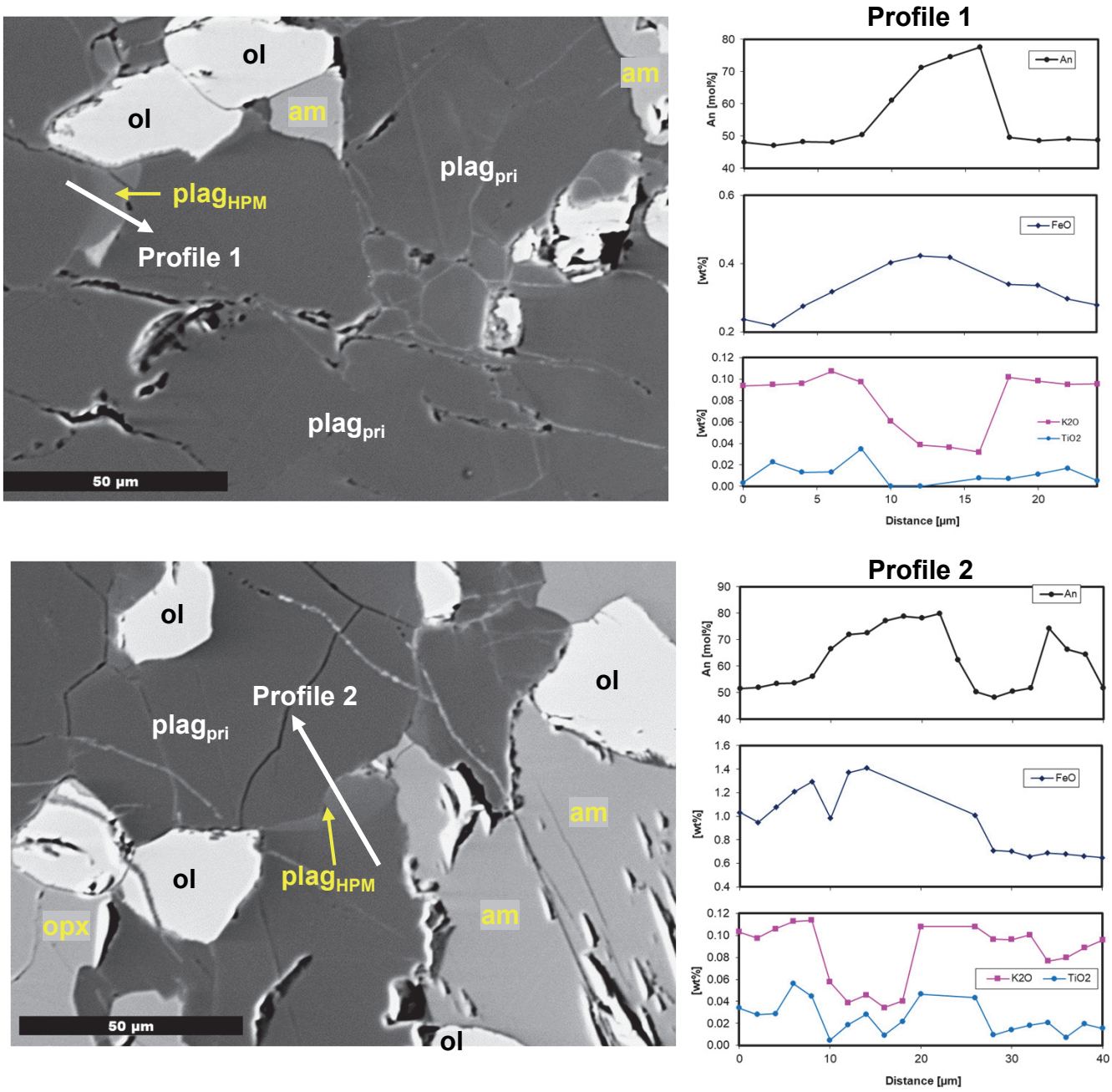

Figure S7. BSE images of zones of An-enriched plagioclases within primary plagioclase, together with two EPMA profiles through such zones in olivine gabbro 149-03-53-61. The An-enriched plagioclase mainly coexists with newly formed pargasite. As usual, the An-enriched part of the profiles is impoverished in TiO_2 and K_2O. The MgO content of the profiles is below the detection limit.

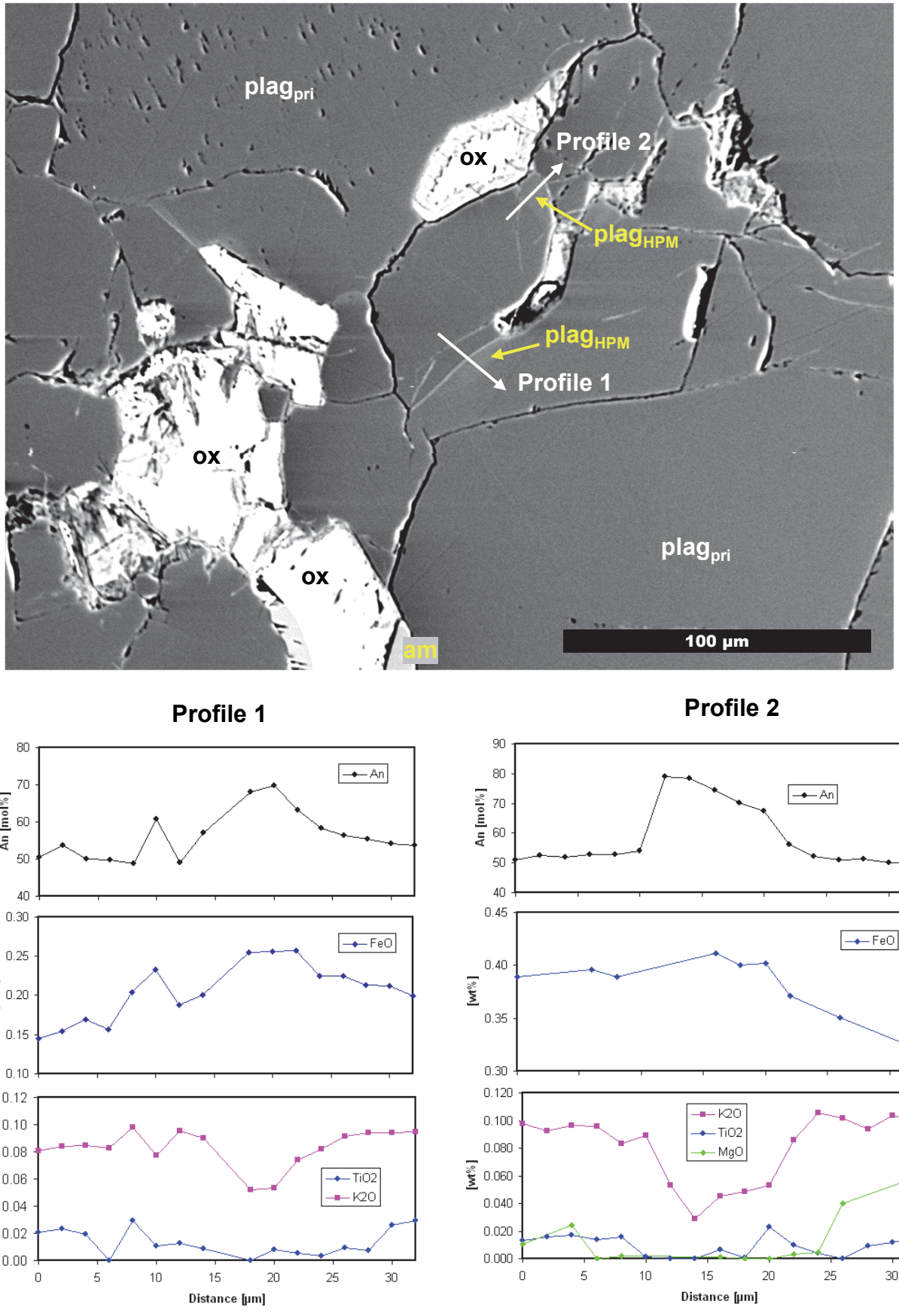

Figure S8. BSE image of zones of newly formed An-enriched plagioclases within primary plagioclase in olivine gabbro 149-03-76-80. Two EPMA profiles across such zones are also shown. The profile for MgO in profile 1 is not shown, since most MgO contents are below detection limit. Coexisting mafic phases are amphiboles of pargasitic compositions (not visible in the BSE image), which are often rimming oxide phases.

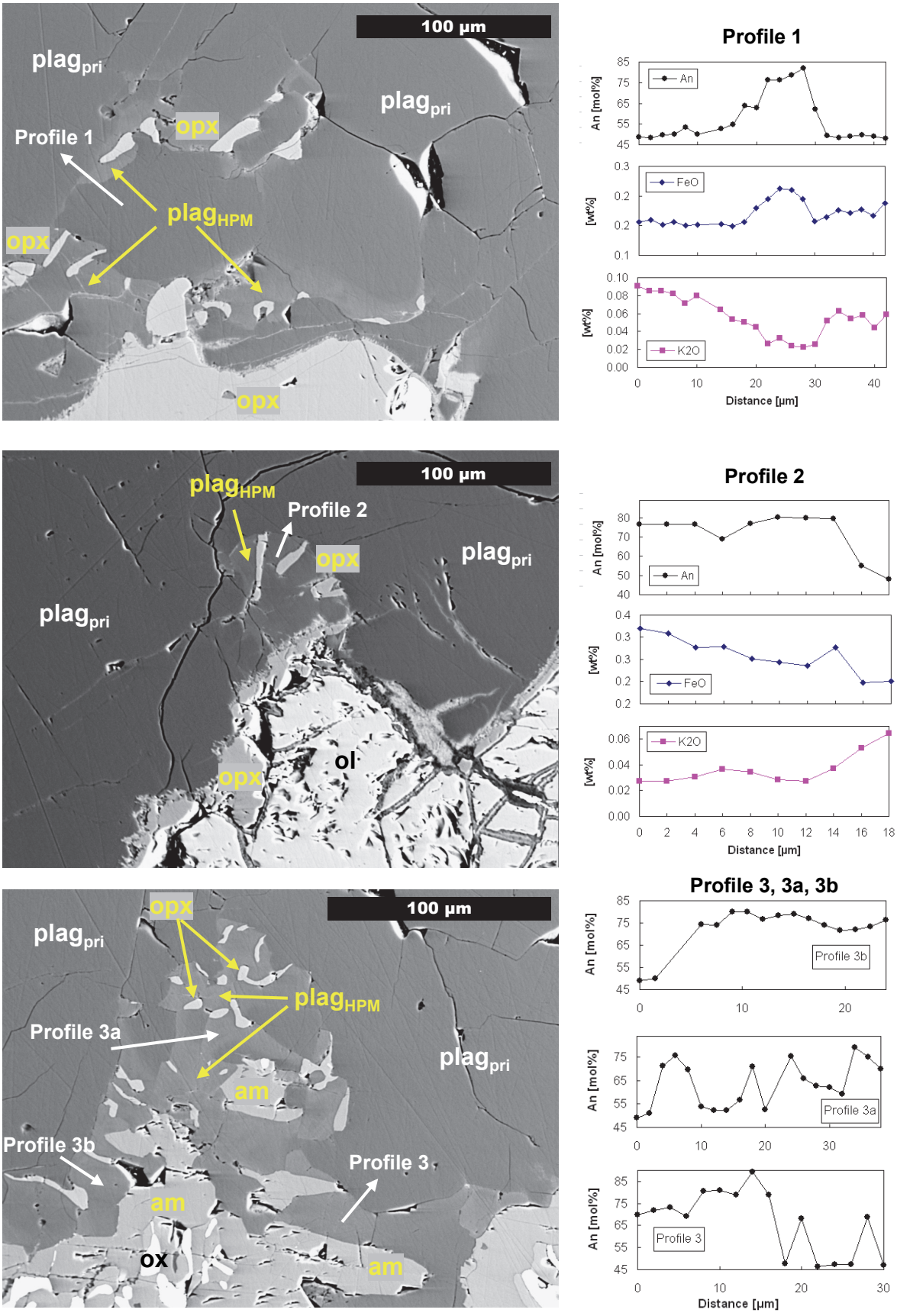

Figure S9. Three BSE images of zones of An-enriched plagioclase from olivine gabbro 157-4-1-9 and related EPMA profiles (MgO and TiO_2 below detection limit). Only the An profiles are shown for three different locations in the lowermost image. The profiles for FeO and K_2O show the same trend: FeO enrichment in the An-rich zone and K_2O impoverishment. The mafic minerals that coexist with the An-enriched plagioclases are magnesio-hastingsite and orthopyroxene. This sample is characterized by symplectitic intergrowth between An-rich plagioclase and orthopyroxene, implying that they formed via reaction instead of simple late-stage crystallization.

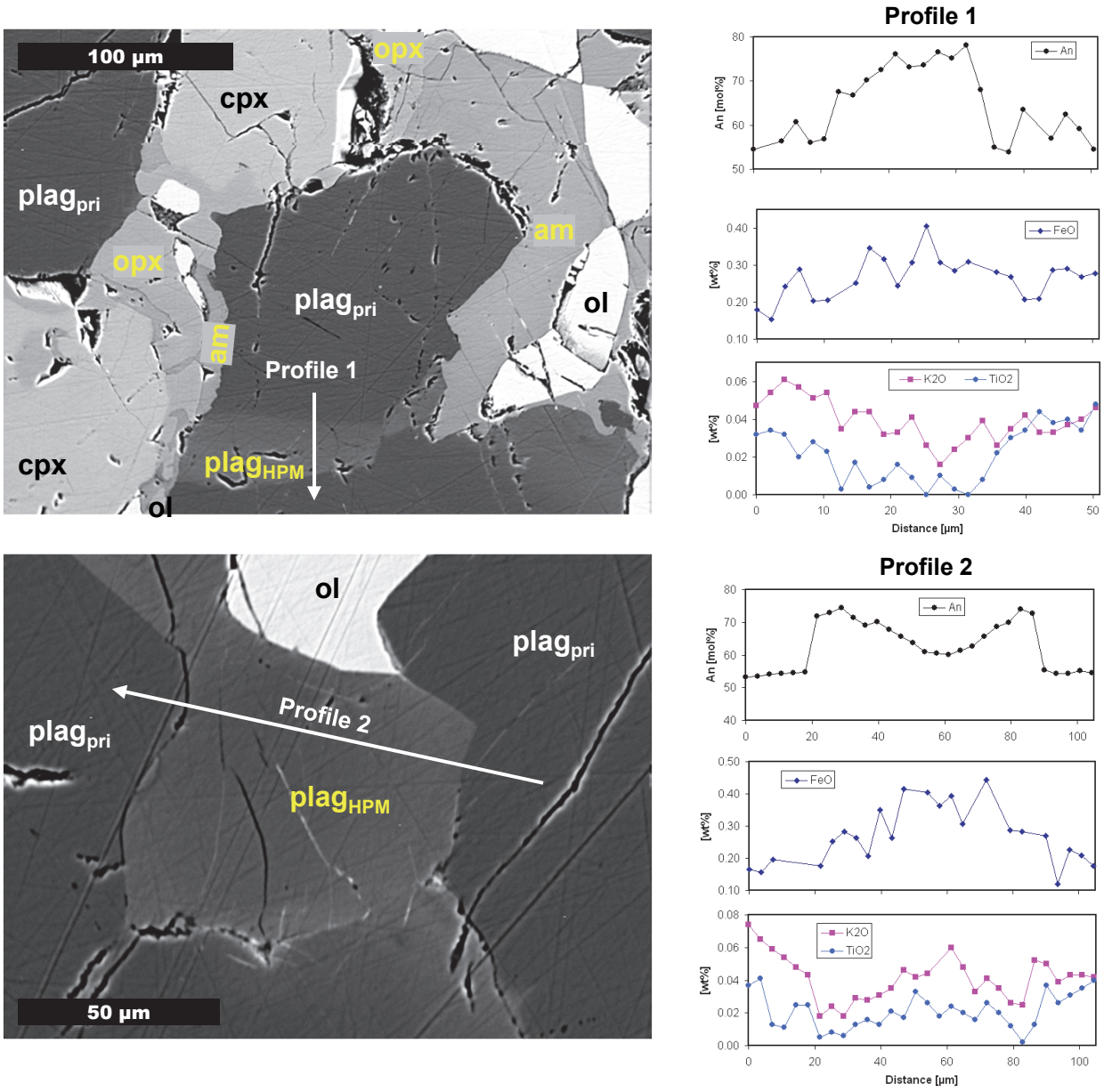

Figure S10. Two BSE images showing zones of newly formed An-enriched plagioclase and related EPMA profiles from olivine gabbro 170-7-50-55. The mafic minerals that coexist with the An-enriched plagioclase are pargasite and orthopyroxene, which are visible in the upper image. The trace element profiles reveal that the An-enriched zones are depleted in trace elements relative to the host plagioclase. This implies that they formed through a 'hydrothermal reaction' rather than by precipitation from a late-stage melt. Reliable MgO profiles could not be obtained due to values below detection limit.

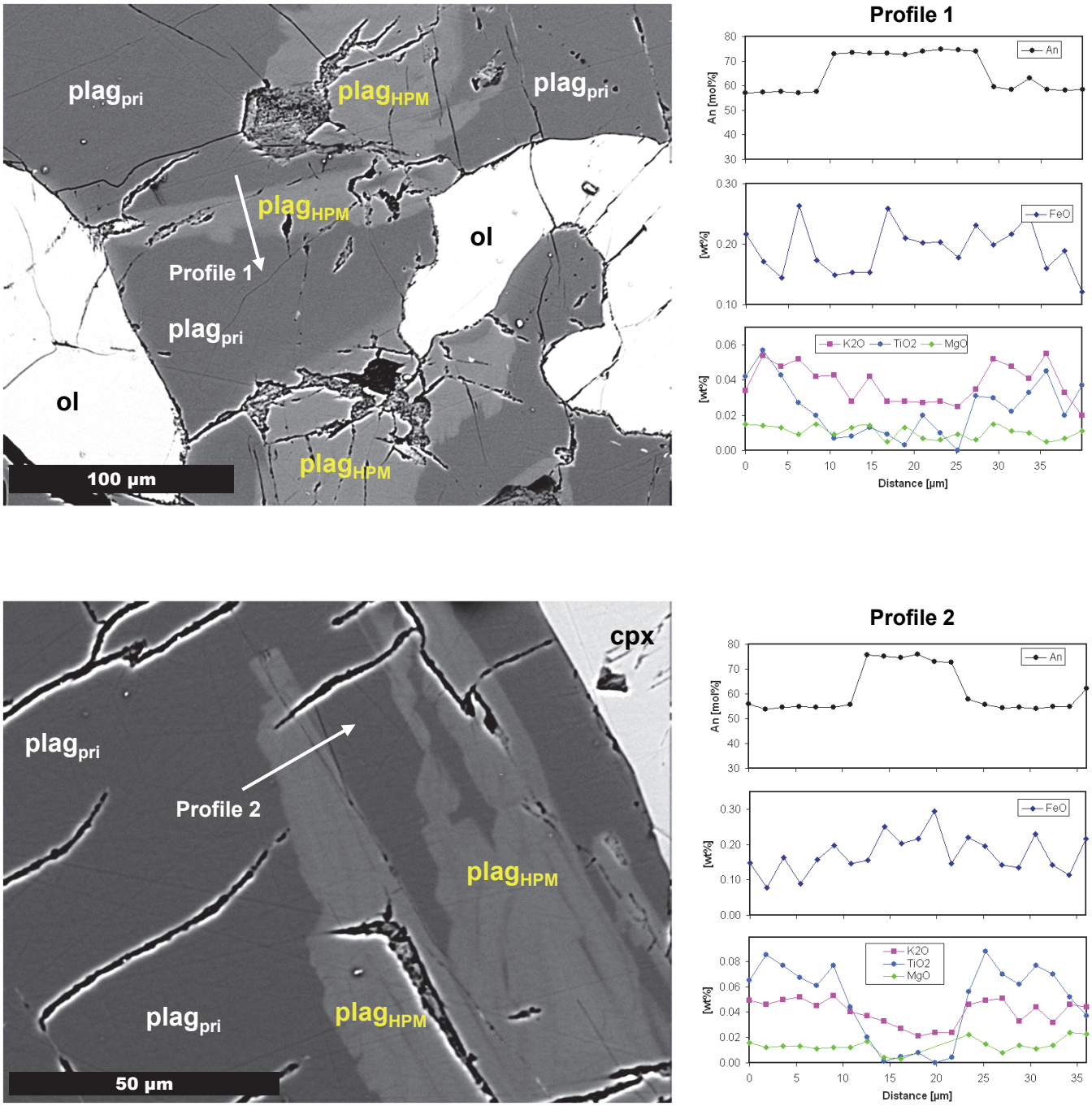

Figure S11. Two BSE images showing zones of An-enriched plagioclase in olivine gabbro 176-6-132-138. The related EPMA profiles show a clear step-like feature: Where the An content is high, the values of MgO, TiO_2 and K_2O are very low. This is not compatible with a model in which the An-rich plagioclase formed from late-stage melts, as TiO_2 and K_2O would be significantly enriched in this case. Instead, a model is favored in which these formations are related to hydrothermal fluids that are characteristically impoverished in trace elements, triggering hydrous partial melting. Note that the An-enriched zones are regions that are strongly affected by low-temperature hydrothermal alteration than the host plagioclase. This implies that the locations influenced by melting are zones of weakness in the rock, since the same pathways were later used for the circulation of hydrothermal fluids at lower temperatures, causing widespread alteration processes.

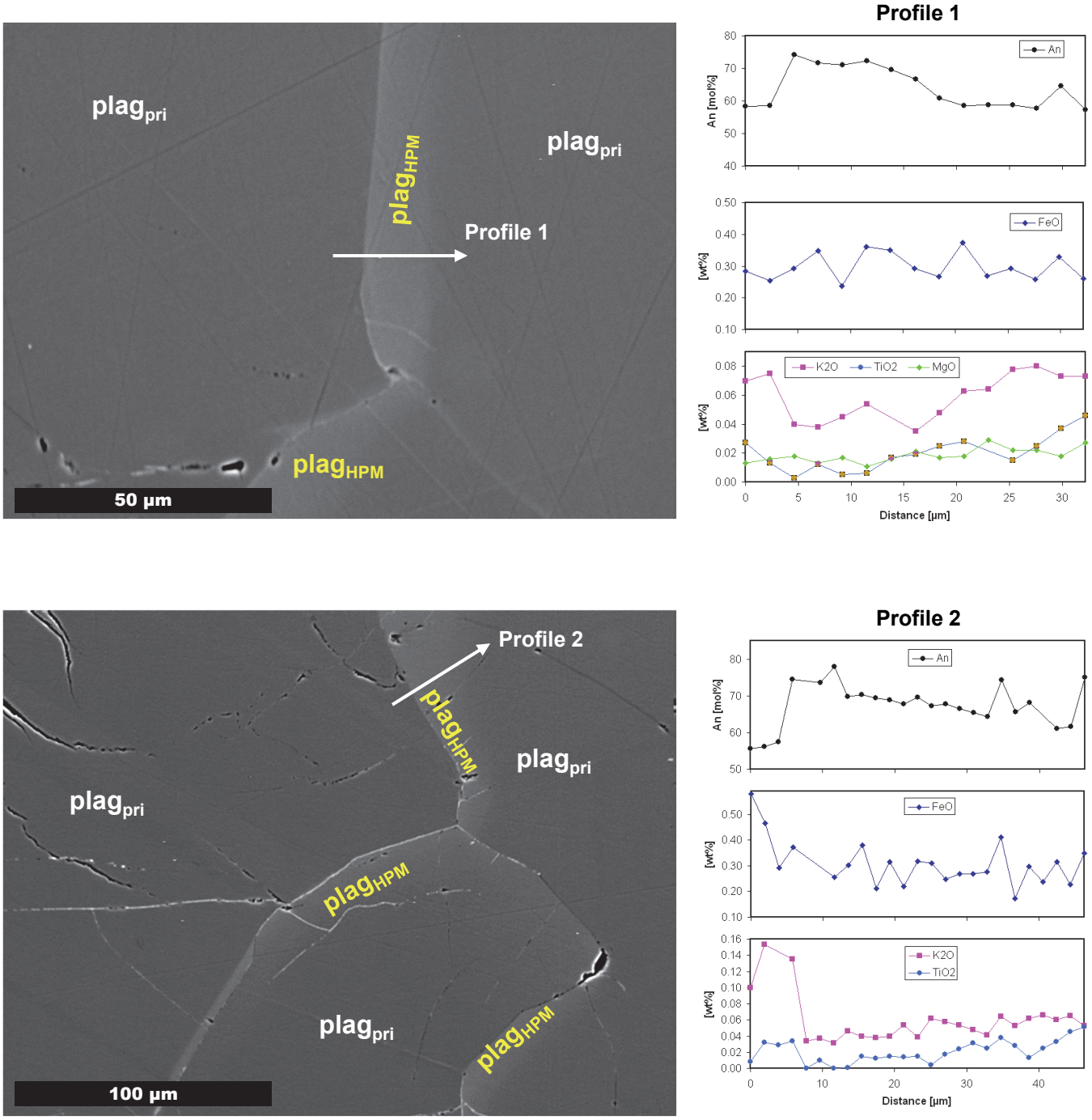

Figure S12. BSE images of zones of newly formed An-rich plagioclase in olivine gabbro 202-8-7-16 and related EPMA profiles are shown. In most analyses of the lower profile, the MgO content is below detection limit. The BSE image clearly shows that the An-rich zones formed at a late stage, following the grain boundary of the primary plagioclase. This implies that they formed when hydrous fluids percolated at very high temperatures along grain boundaries, triggering hydrous partial melting. Three additional profiles (not shown here) performed on the lower image yielded identical results.

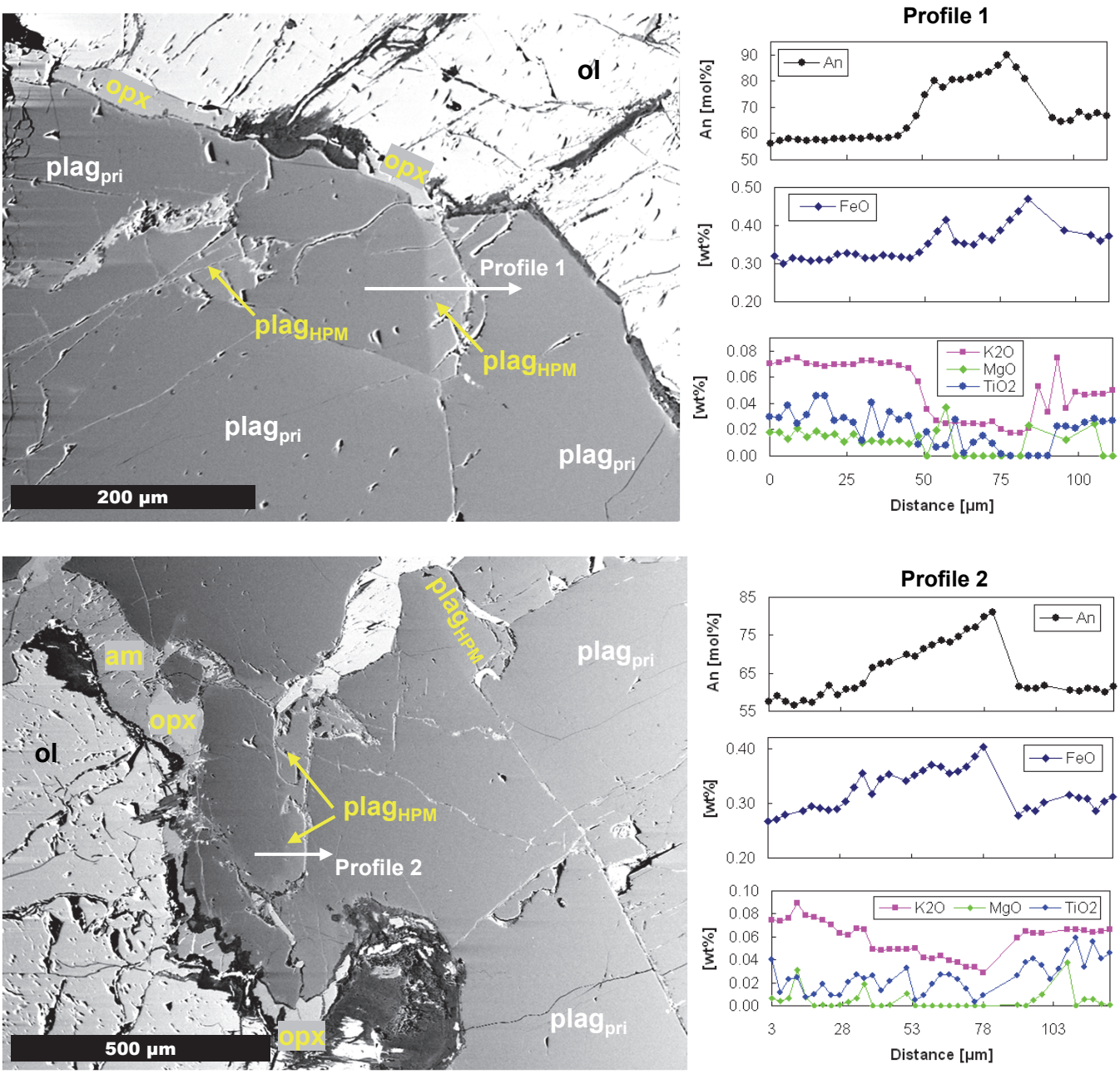

Figure S13. Two BSE images showing zones of An-enriched plagioclase in olivine gabbro 206-2-46-52. The orthopyroxene and pargasite form rims around the primary olivine (and clinopyroxene) and are often characteristically linked via grain boundaries with the zones of An-enriched plagioclase. This implies that these phases were formed by the same reactive process: hydrous partial melting, triggered by water-rich fluids percolating along grain boundaries at temperatures above the wet gabbro solidus. The formation temperature of an average pargasite within this sample was estimated to be 900°C using the Ti-in-amphibole geothermometer of Ernst and Liu (1998).

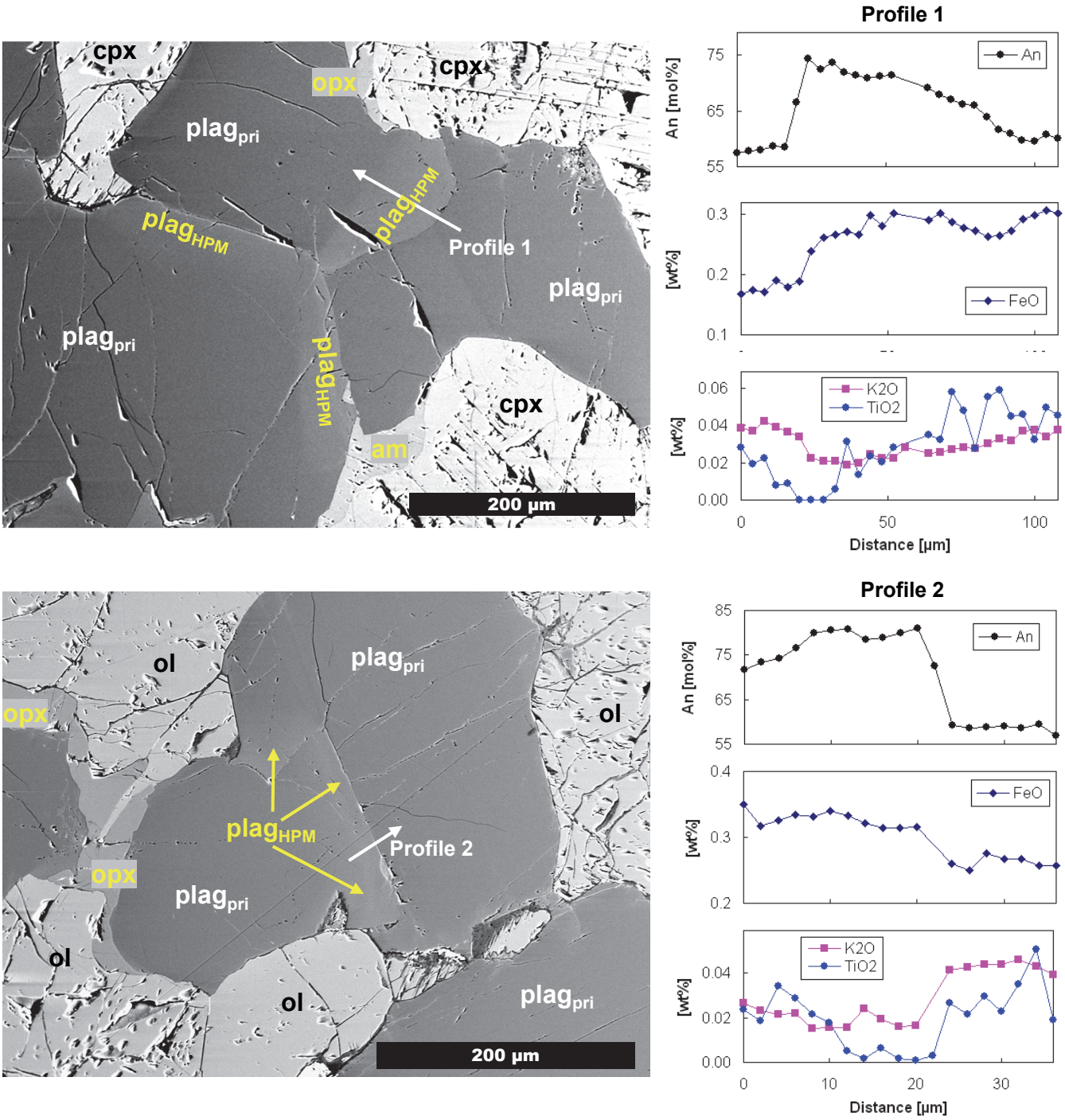

Figure S14. BSE images of zones of newly formed An-enriched plagioclase in olivine gabbro 207-4-64-70, alongside related EPMA profiles (MgO below the detection limit). The coexisting mafic phases are amphibole (magnesio-hastingsite) and/or orthopyroxene. The petrographic record suggests formation by hydrous partial melting, analogous to the experiments of Wolff et al. (2013).